International Journal of Bifurcation and Chaos, Vol. 3, No. 1 (1993) 19–34

HIGHER-ORDER SPECTRAL ANALYSIS TO DETECT NONLINEAR INTERACTIONS IN MEASURED TIME SERIES AND AN APPLICATION TO CHUA'S CIRCUIT

STEVE ELGAR and VINOD CHANDRAN
School of Electrical Engineering and Computer Science, Washington State University, Pullman, WA 99164-2752, USA

Received December 8, 1992

Higher-order spectra have been used to investigate nonlinear interactions between the Fourier components of measured time series in a remarkably wide range of random processes. The basic techniques of detecting and isolating nonlinear phase coupling in observed data using higher-order spectral analysis are reviewed here. These techniques are then used to investigate nonlinear interactions in time series of voltages measured from a realization of Chua's circuit. For period-doubled limit cycles, quadratic and cubic nonlinear interactions result in phase coupling and energy exchange between increasing numbers of triads and quartets of Fourier components as the nonlinearity of the system is increased. For circuit parameters that result in a chaotic, Rössler-type attractor, bicoherence and tricoherence spectra indicate that both quadratic and cubic nonlinear interactions are important to the dynamics. For parameters that lead to the double-scroll chaotic attractor the bispectrum is zero, but the tricoherences are high, consistent with the importance of higher-than-second order nonlinear interactions during chaos associated with the double scroll.

1. Introduction

Since their introduction thirty years ago [Hasselmann *et al.*, 1963], higher-order spectral techniques, which isolate nonlinear interactions between the Fourier components of a time series, have been used to study many systems. One of the purposes of the present study is to review the development of higher-order spectral analysis techniques since the seminal work of Hasselmann *et al.* [1963], with special emphasis on the detection of nonlinearly induced phase coupling between the Fourier components of measured (i.e., observed) time series. First, the basic techniques of higher-order spectral analysis will be reviewed by examining numerically simulated quadratic and cubic nonlinear systems. Although the application of higher-order spectral analysis (in particular, the bispectrum) to quadratically nonlinear systems is well known, trispectral analysis has not yet been applied to many measurements, and some new methodology is presented here. The statistics of estimates of higher-order spectra obtained from finite-length and/or noisy measurements are only briefly discussed, with some references provided for further reading. Once the basic techniques have been reviewed, they will be used to investigate the nonlinear interactions between triads and quartets of Fourier components of voltages measured in the Chua circuit as it undergoes a period-doubling cascade to chaos.

The earliest time series analyses consisted primarily of time-domain statistics such as the mean and variance. Deviations from Gaussianity were quantified by the skewness and kurtosis. Additional information about the time series is provided by the power spectrum, which gives the distribution of variance as a function of frequency. However,

the power spectrum has no phase information, and thus is not sufficient for describing a nonlinear time series, where Fourier components are not random relative to each other, but interact and become phase coupled.

The importance of phase has been utilized in dynamical systems analysis to investigate nonlinear processes. Phase space portraits and other phase-retaining descriptions of the time series have led to quantitative measures of nonlinear systems such as the fractal dimension, including the Grassberger–Procaccia, or correlation dimension [Grassberger & Procaccia, 1983a, 1983b; Roux *et al.*, 1983], the averaged pointwise dimension [Farmer *et al.*, 1983], and the Lyapunov dimension [Frederickson *et al.*, 1983]. Along with dimension, numerically generated or experimentally observed time series can be characterized by power spectra, phase space portraits, Poincaré sections, and Lyapunov exponents [Packard *et al.*, 1980; Wolf *et al.*, 1985; Brandstater & Swinney, 1987; and many others].

Although these methods of modern nonlinear dynamics have been extremely valuable for investigating nonlinear systems, they do not present direct information about nonlinear interactions between the Fourier components of the system. On the other hand, higher-order spectral analysis specifically isolates and quantifies the nonlinearly induced phase coupling between Fourier modes, and thus provides information in addition to that given by bulk statistics of the time series (e.g., variance), the power spectrum, or dimension estimates.

Bispectral analysis isolates the nonlinearly-induced phase coupling between triads of Fourier modes in quadratically nonlinear systems. This phase coupling can lead to cross-spectral transfers of energy (e.g., growth of super and/or subharmonics) and to non-Gaussian statistics (e.g., non-sinusoidal wave profiles). Bispectral analysis has been used to study quadratic nonlinear interactions observed in many nonlinear systems, including economic [Godfrey, 1965; Hinich & Patterson, 1989], biological [Barnett *et al.*, 1971; Huber *et al.*, 1971], fluid [Yeh & Van Atta, 1973; Lii *et al.*, 1976; Helland *et al.*, 1977; Van Atta, 1979; Herring, 1980; Miksad *et al.*, 1983; Ritz *et al.*, 1988; Hajj *et al.*, 1992], plasma [Kim & Powers, 1978, 1979; Kim *et al.*, 1980; Arter & Edwards, 1986], oceanographic [Hasselmann *et al.*, 1963; Rodin & Bendiner, 1973; Neshyba & Sobey, 1975; McComas & Briscoe, 1980; Masuda & Kuo, 1981a, b; Elgar & Guza, 1985; Herbers & Guza, 1992; Herbers *et al.*, 1992; Herbers *et al.*, 1993], geophysical [Haubrich, 1963; Hinich & Clay, 1965], acoustical [Hinich *et al.*, 1989], astronomical [Lohmann *et al.*, 1983; Bartelt & Wirnitzer, 1985], mechanical [Sato *et al.*, 1977; Pezeshki *et al.*, 1990; Pezeshki *et al.*, 1991; Chandran *et al.*, 1993a], coupled fluid-mechanical [Choi *et al.*, 1985; Elgar *et al.*, 1990; Miles *et al.*, 1992], quantum-mechanical [Miller, 1986], paleoclimatological [Hagelberg *et al.*, 1991], electrical [Elgar & Kennedy, 1993], and many other systems.

Trispectral analysis isolates the nonlinearly induced phase coupling between quartets of Fourier modes in cubically nonlinear systems, and has only recently been applied to observations of nonlinear systems [Dalle Molle & Hinich, 1989; Dwyer, 1984, 1989; Lutes & Chen, 1991; Dalle Molle, 1992; Chandran *et al.*, 1993b].

The references cited above are only a few of the many applications of higher-order spectral analysis to observations of nonlinear systems. There is also a rich literature on other uses of higher-order spectral analysis, including system identification and signal reconstruction. These are not discussed here, but reviews are given by Nikias & Raghuveer [1987], Mendel [1991], and references therein.

Definitions and properties of higher-order spectra, in particular bispectra and trispectra are presented in Sec. 2, where examples of quadratic and cubic nonlinear systems are studied in detail. In Sec. 3 higher-order spectral analysis is used to investigate the nonlinear interactions between triads and quartets of Fourier components in voltages measured in a realization of the Chua circuit as it undergoes a period-doubling cascade to chaos. Previous studies indicate that although quadratic interactions are important for the limit cycles preceeding chaos, higher-order nonlinear interactions often dominate the dynamics in chaos [Miller, 1986; Elgar *et al.*, 1989; Pezehski *et al.*, 1990; Elgar & Kennedy, 1993; Chandran *et al.*, 1993b, and others]. Consequently, both bispectral and trispectral analysis of the Chua circuit are presented in Sec. 3. Conclusions follow in Sec. 4.

2. Definitions, Properties, and Examples of Higher-Order Spectra

Let a stationary random process be represented as

$$\eta(t) = \sum_{n=1}^{N} A_n e^{i\omega_n t} + A_n^* e^{-i\omega_n t}\,, \qquad (1)$$

where t is time, ω is the radian frequency, the subscript n is a frequency (modal) index, asterisk indicates complex conjugation, and the A_n are complex Fourier coefficients. The auto-bispectrum is formally defined as the Fourier transform of the third-order correlation function of the time series [Hasselmann *et al.*, 1963]

$$B(\omega_1, \omega_2) = \left(\frac{1}{2\pi}\right)^2 \int_{-\infty}^{\infty}\int_{-\infty}^{\infty} S(\tau_1, \tau_2) \times e^{i\omega_1\tau_1 - i\omega_2\tau_2} d\tau_1 d\tau_2 , \quad (2)$$

$$\text{where} \quad S(\tau_1, \tau_2) = E[\eta(t)\eta(t+\tau_1)\eta(t+\tau_2)] \quad (3)$$

with $E[\cdot]$ the expected-value, or average, operator. The discrete bispectrum, appropriate for discretely sampled data, is [Haubrich, 1965; Kim & Powers, 1979]

$$B(\omega_1, \omega_2) = E[A_{\omega_1} A_{\omega_2} A^*_{\omega_1+\omega_2}] . \quad (4)$$

Similarly, the power spectrum is defined here as

$$P(\omega_1) = \frac{1}{2} E[A_{\omega_1} A^*_{\omega_1}] . \quad (5)$$

From Eq. (4) the bispectrum is zero if the average triple product of Fourier coefficients is zero. This occurs if the Fourier components are independent of each other, i.e., for the random phase relationships between Fourier modes in a linear process, such as a time series with Gaussian statistics. Using symmetry properties of Fourier transforms of discrete-time, real-valued processes, the bispectrum can be shown to be uniquely described by its values in a bifrequency octant. For a discrete time series with Nyquist frequency ω_N, the bispectrum is uniquely defined within a triangle in (ω_1, ω_2)-space with vertices at $(\omega_1 = 0, \omega_2 = 0)$, $(\omega_1 = \omega_{N/2}, \omega_2 = \omega_{N/2})$, and $(\omega_1 = \omega_N, \omega_2 = 0)$.

It is convenient to recast the bispectrum into its normalized magnitude and phase, called the squared bicoherence and biphase, given respectively by [Kim & Powers, 1979]

$$b^2(\omega_1, \omega_2) = \frac{|B(\omega_1, \omega_2)|^2}{E[|A_{\omega_1} A_{\omega_2}|^2] E[|A_{\omega_1+\omega_2}|^2]} , \quad (6)$$

$$\beta(\omega_1, \omega_2) = \arctan\left[\frac{-\text{Im}\{B(\omega_1, \omega_2)\}}{\text{Re}\{B(\omega_1, \omega_2)\}}\right] . \quad (7)$$

For a three-wave system, Kim & Powers [1979] show that $b^2(\omega_1, \omega_2)$ represents the fraction of power at frequency $\omega_1 + \omega_2$ owing to quadratic coupling of the three modes (ω_1, ω_2, and $\omega_1 + \omega_2$). No such simple interpretation for the bicoherence is possible in a broad-band process where a particular mode may be simultaneously involved in many interactions [McComas & Briscoe, 1980]. Nevertheless, the bicoherence does give an indication of the relative degree of phase coupling between triads of Fourier components, with $b = 0$ for random phase relationships, and $b = 1$ for maximum coupling.

The biphase is related to the shape (in a statistical sense) of the time series [Masuda & Kuo, 1981a; Elgar, 1987].

Cross bispectra between time series simultaneously measured at more than one spatial location or between colocated, simultaneous time series of different variables are defined similar to the auto-bispectrum [Eq. (4)], with the complex Fourier coefficients (A_{ω_n}) of the different time series used in the expected value operation. Cross bispectra have been used to study the coupling between temperature, salinity, and density in the ocean [Rodin & Bendiner, 1973], turbulent flows [Lii & Helland 1981], waves in different locations near the beach [Elgar & Guza, 1985], ship motions and ocean waves [Choi *et al.*, 1985], a cylinder and its wake in laminar flow [Elgar *et al.*, 1990], beam vibrations and external forces [Pezeshki *et al.*, 1992], and other systems. Similarly, bispectra can be defined for two-dimensional random processes and have been used to detect 2-D quadratic phase coupling in measured spatial series in astronomy [Bartlet & Wirnitzer, 1985], ocean waves [Chandran & Elgar, 1990; Herbers *et al.*, 1993], pattern recognition [Raghuveer & Dianat, 1988; Sadler, 1989; Chandran & Elgar, 1993a], and other random processes.

Consider the time series given by

$$\eta(t) = \cos(\omega_1 t + \theta_1) + \cos(\omega_2 t + \theta_2) + \cos(\omega_3 t + \theta_3) + n(t) \quad (8)$$

where $\omega_3 = \omega_1 + \omega_2$ and $\omega_1 = 2\pi(0.0625)$, $\omega_2 = 2\pi(0.1875)$, $\omega_3 = 2\pi(0.2500)$, θ_i is the phase of each Fourier component and $n(t)$ is low level (less than 2% of the total variance) background Gaussian noise. If the three Fourier phases are independent and randomly distributed in $[0, 2\pi)$ (Case A), then a time series consisting of many realizations with different sets of random phases will have Gaussian statistics. The power spectrum of such a time series is shown in Fig. 1, and one realization of the time series is shown in Fig. 2a. Since

the Fourier phases are independent of each other, $b(f_1, f_2) = 0$ (where $f = \omega/(2\pi)$ and $f_1 = .0625$, $f_2 = .1875$ Hz), as shown in Fig. 3a. In this case the biphase, $\beta(f_1, f_2)$ is undefined and is distributed between $\pm\pi$.

If θ_1 and θ_2 are randomly distributed in $[0, 2\pi)$ and $\theta_3 = \theta_1 + \theta_2$, then although each of the three Fourier phases is randomly distributed, the *phase relationship* between the three Fourier components is not random, and the biphase is $\beta(f_1, f_2) = \theta_3 - (\theta_1 + \theta_2) = 0$. Such a phase relationship occurs in a quadratic interaction between the components at frequencies f_1 and f_2 and their multiplicative sum frequency, f_3. In this case (B), although the time series has the identical power spectrum as in Case A (Fig. 1), it does not have Gaussian statistics [Fig. 2(b)], and $b(f_1, f_2) > 0$ [Fig. 3(b)]. In the absence of noise and for $\eta(t)$ infinitely long, $b(f_1, f_2) = 1.0$. The low level background noise reduces slightly the value of the bicoherence by introducing some random (i.e., independent) components at each frequency.

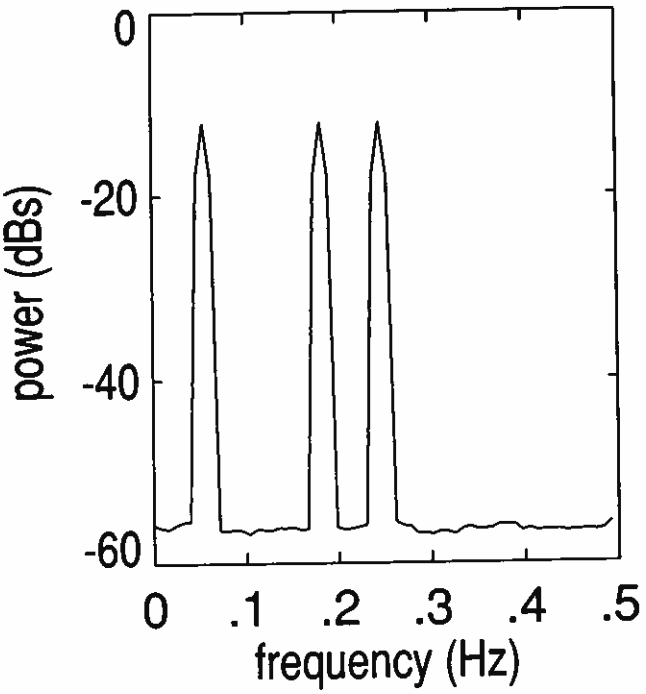

Fig. 1. Power spectrum for the time series of Example 1 (Eqs. (8)–(9)). Despite the differences in the time series owing to different phase relationships (see text), the power spectra for each case are identical.

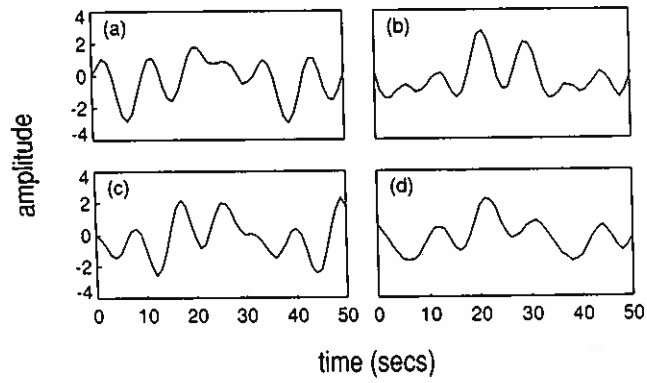

Fig. 2. Amplitude versus time for short sections of the four time series of Example 1. (a) random phase, (b) phase coupled, $\beta = 0$, (c) phase coupled, $\beta = -\pi/2$, (d) partially phase coupled. (See text for a complete description.)

If θ_1 and θ_2 are randomly distributed in $[0, 2\pi)$ and $\theta_3 = \theta_1 + \theta_2 + \pi/2$ (Case C), the power (Fig. 1) and bicoherence spectra [Fig. 3(c)] are identical to Case B [Fig. 3(b)], but $\beta(f_1, f_2) = -\pi/2$, and the time series has a different shape [Fig. 2(c)] than when $\beta(f_1, f_2) = 0$. Unlike a Gaussian process, time series with $\beta(f_1, f_2) = 0$ have nonzero skewness (the mean of the cube of the time series, normalized by the variance), and are characterized by wave profiles that have sharp peaks, and broad, flat troughs [an asymmetry with respect to a horizontal axis, Fig. 2(b)]. As shown by Hasslemann *et al.* [1963] the distribution of third moments in bifrequency space is given by the bispectrum, similar to the distribution of variance given by the power spectrum. The skewness is the sum of the real parts of the bispectrum. For a time series with $\beta(f_1, f_2) = -\pi/2$, the skewness is zero, but the time series is asymmetrical with respect to a vertical axis [e.g., $20 <$ time < 35 in Fig. 2(c)], and is characterized by fore-aft asymmetric wave forms (e.g., the steep front faces and gently sloping rear faces of nearly breaking ocean waves) [Masuda & Kuo, 1981a; Elgar & Guza, 1985; Elgar, 1987]. A quantity analogous to skewness, called the asymmetry is the sum of the imaginary parts of the bispectrum (asymmetry is the skewness of the Hilbert transform (a phase shift by $\pi/2$) of the time series [Elgar & Guza, 1985; Elgar, 1987]).

In general, the Fourier components of a nonlinear random process are partially coupled, as opposed to the complete coupling (neglecting the additive noise) in the cases discussed above. If the Fourier component of the sum frequency (ω_3) of the example time series in Eq. (8) is given by

$$\cos(\omega_3 t + \theta_3) = \hat{b}\cos(\omega_3 t + \theta_{3c}) + \sqrt{1 - \hat{b}^2}\cos(\omega_3 t + \theta_{3r}), \quad (9)$$

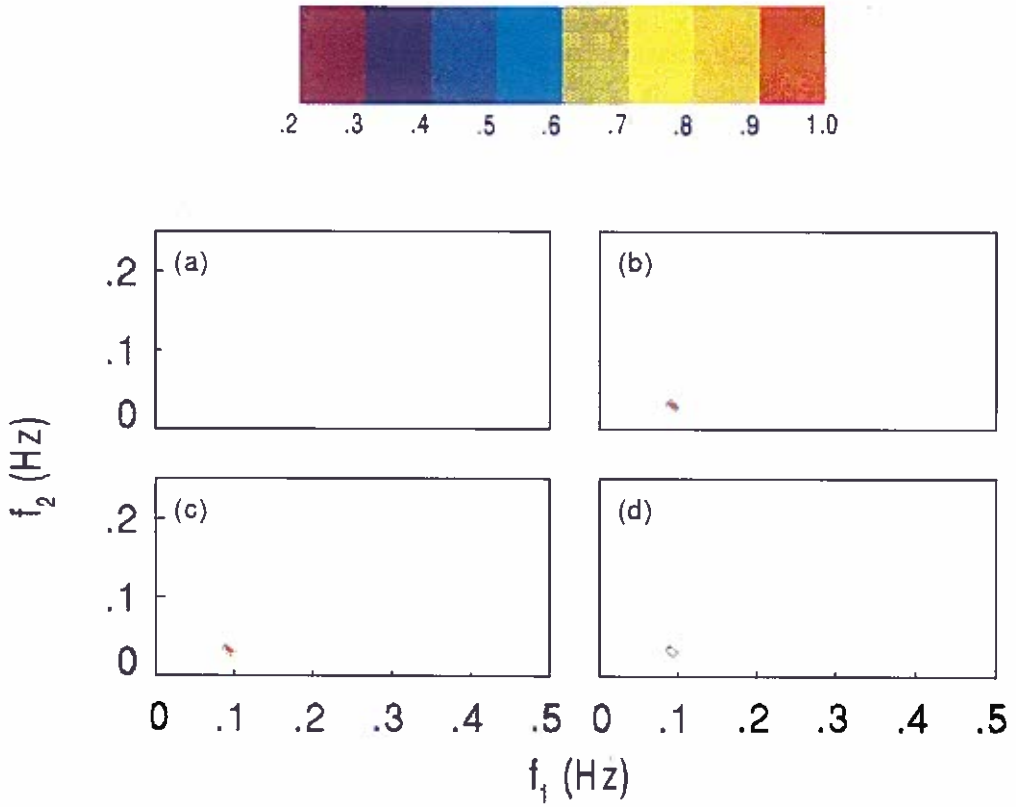

Fig. 3. Bicoherence spectra for the time series of Example 1. Color contours indicate quadratic phase coupling between motions with frequencies f_1, f_2, $f_1 + f_2$. The minimum contour plotted is $b = 0.2$ and the scale for the contours is given by the color bar at the top of the figure. This scale is used in all subsequent color figures. (a) random phase, (b) phase coupled, $\beta = 0$, (c) phase coupled, $\beta = -\pi/2$, (d) partially phase coupled.

where $\theta_{3c} = \theta_1 + \theta_2$, θ_{3r} is randomly distributed, and $\hat{b} = 0.8$, then at frequency ω_3 the time series contains both a coupled triad of Fourier components (with phases θ_1, θ_2, θ_{3c}) and a random component (with phase θ_{3r}). The bicoherence (in the absence of noise) is $b(f_1, f_2) = 0.8$, and is only slightly reduced by the background noise, as shown in Fig. 3(d). The power spectrum (Fig. 1) remains identical to the other three cases and the time series [Fig. 2(d)] is non-Gaussian.

Similar to the bispectrum, the auto-trispectrum is formally defined as the Fourier transform of the fourth-order auto-correlation. The discrete trispectrum is thus

$$T(\omega_1, \omega_2, \omega_3) = E[A_{\omega_1} A_{\omega_2} A_{\omega_3} A^*_{\omega_1+\omega_2+\omega_3}]. \quad (10)$$

The normalized magnitude and phase of the trispectrum are known as the squared tricoherence, t^2 and triphase, respectively, where (see Chandran *et al.* [1993a] for alternative normalizations)

$$t^2(\omega_1, \omega_2, \omega_3) = \frac{|T(\omega_1, \omega_2, \omega_3)|^2}{E[|A_{\omega_1} A_{\omega_2} A_{\omega_3}|^2] E[|A_{\omega_1+\omega_2+\omega_3}|^2]}, \quad (11)$$

The tricoherence is a measure of the fraction of the power of the quartet of Fourier components $(\omega_1, \omega_2, \omega_3, \omega_{1+2+3})$ that is owing to cubic nonlinear interactions.

Owing to symmetry relations, the trispectrum need be calculated only in a subset of the complete $(\omega_1, \omega_2, \omega_3)$-space. For sum interactions, this reduced region of computation is a tetrahedron with base (lying on the plane $\omega_3 = 0$) equal to the triangle given above for the region of computation of the bispectrum and with apex given by $(\omega_1 = \omega_N/3, \omega_2 = \omega_N/3, \omega_3 = \omega_N/3)$. For difference interactions an additional region is necessary (Chandran & Elgar, 1993b). These regions assume there is no spectral aliasing (i.e., the time series has no energy above frequency $= \omega_N$). Complete descriptions of nonredundant regions of computation for general higher-order spectra are given by Dalle Molle [1992] and Chandran & Elgar [1993b]. In many cases, the sum interactions are sufficient, and the display of the tricoherence (which is a function of three variables) can be simplified and shown as contours drawn in the two-dimensional (ω_1, ω_2)-space for fixed values of the sum frequency, $\omega_4 =$

$\omega_1 + \omega_2 + \omega_3$, as shown in Fig. 4. By repeating for different values of ω_4, all the information contained in the trispectrum is displayed. In the example display (Fig. 4) $\omega_4 = 0.75$, and given any point in the figure (i.e., given values for ω_1 and ω_2), ω_3 is uniquely determined. The point labelled A in Fig. 4 corresponds to the quartet consisting of $(\omega_1 = \omega_2 = \omega_3 = \omega_4/3)$. Along the line from point A to point B, $\omega_1 = \omega_2$, and $\omega_3 = \omega_4 - 2\omega_1$. Point B corresponds to $\omega_1 = \omega_2 = \omega_4/2$ and $\omega_3 = 0$. From point B to point C, $\omega_3 = 0$ and $\omega_2 = \omega_4 - \omega_1$. At point C, $\omega_2 = \omega_3 = 0$ and $\omega_1 = \omega_4$. Between point C and point A, $\omega_2 = \frac{1}{2}(\omega_4 - \omega_1)$ and $\omega_3 = \omega_2$. Lines parallel to $\overline{BC}$ have $\omega_1 + \omega_2 =$ constant and thus the line $\overline{AB}$ can serve as an ω_3 axis.

Consider the time series given by

$$\begin{aligned}\eta(t) = &\cos(\omega t + \theta_1) + \hat{b}\cos(2\omega t + 2\theta_1) \\ &+ \sqrt{1-\hat{b}^2}\cos(2\omega t + \theta_{2r}) + \hat{t}\cos(3\omega t + 3\theta_1) \\ &+ \sqrt{1-\hat{t}^2}\cos(3\omega t + \theta_{3r} + n(t)), \end{aligned} \tag{12}$$

where θ_1, θ_{2r}, and θ_{3r} are uniformly distributed in $[0, 2\pi)$, and $\omega = 2\pi(0.0625)$. The corresponding power spectrum is shown in Fig. 5. Thus, $\eta(t)$ consists primarily of three Fourier components, whose dependence on each other is given by the values of $\hat{b}$ and $\hat{t}$. If $\hat{b} = \hat{t} = 0$ then, when averaged over many realizations of the random process, the Fourier components are statistically independent and both the bicoherence and tricoherence are zero, as shown in Figs. 6(a) and 7(a). If $\hat{b} = 0.9$ and $\hat{t} = 0$, the process consists of a triad of quadratically phase coupled components $(f_1, f_1, 2f_1)$, but no cubically coupled components. Thus, $b(f_1, f_1) = 0.9$ [Fig. 6(b)] and the tricoherence = 0 [Fig. 7(b)]. On the other hand,

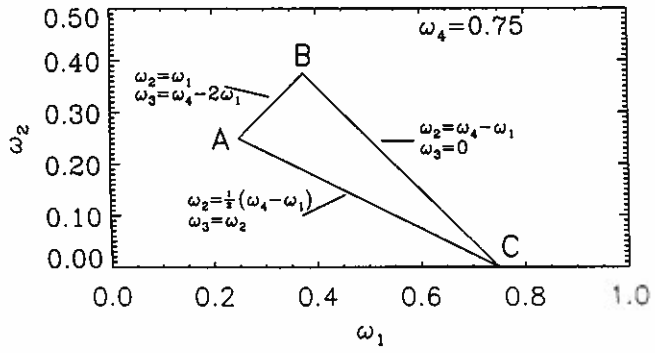

Fig. 4. The nonredundant region of computation of the tricoherence for sum interactions ($\omega_4 = \omega_1 + \omega_2 + \omega_3$, and all frequencies are greater than zero) for a particular (constant) ω_4 ($\omega_4 = 0.75$ in the figure).

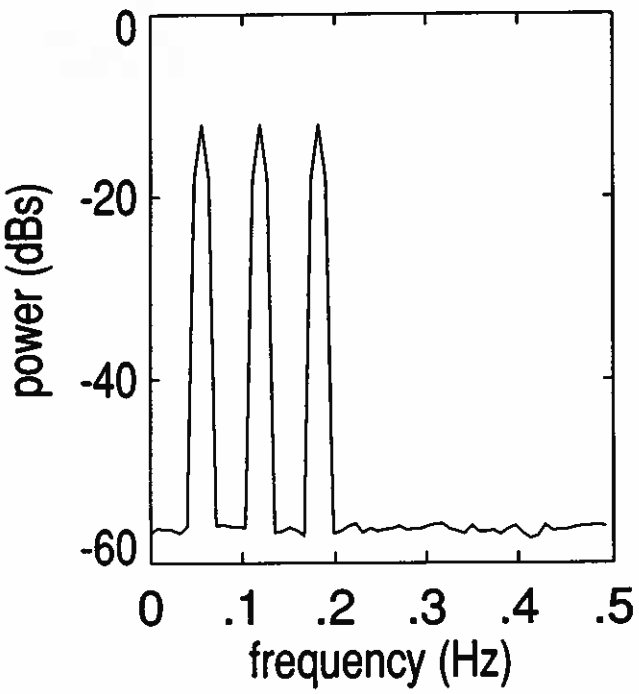

Fig. 5. Power spectrum for the time series of Example 2 [Eq. (12)]. Despite the differences in the time series (see text), the power spectra for each case are identical.

if $\hat{b} = 0$ and $\hat{t} = 0.9$ the process has no quadratically coupled components [Fig. 6(c)], but contains a cubically phase coupled quartet and $t(f_1, f_1, f_1) = 0.9$ [Fig. 7(c)]. If $\hat{b} = \hat{t} = 0.9$, there are two quadratically coupled triads [f_1, f_1, $2f_1$, and f_1, $2f_1$, $3f_1$, Fig. 6(d)] and a cubically coupled quartet [f_1, f_1, f_1, $3f_1$, Fig. 7(d)].

For the examples discussed above, the background noise level is low, and reduces only slightly the observed bicoherence and tricoherence from the noise-free values. Many observed time series have significantly larger background noise levels, but higher-order spectra are zero for nonphase-coupled Fourier components, including components with power owing to random noise. Thus, higher-order spectral analysis can detect even relatively weak nonlinear phase coupling in the presence of linear components and/or significant noise. However, to determine if observed values of higher-order coherences are significant (as opposed to being the result of statistical fluctuations) the statistics of estimates of higher-order spectra must be known. For example, even a truly Gaussian process will have a nonzero higher-order spectrum if a finite-length time series is examined. Beginning with Brillinger [1965], Rosenblatt & Van Ness [1965], and Brillinger & Rosenblatt [1967a, b] there have been many stud-

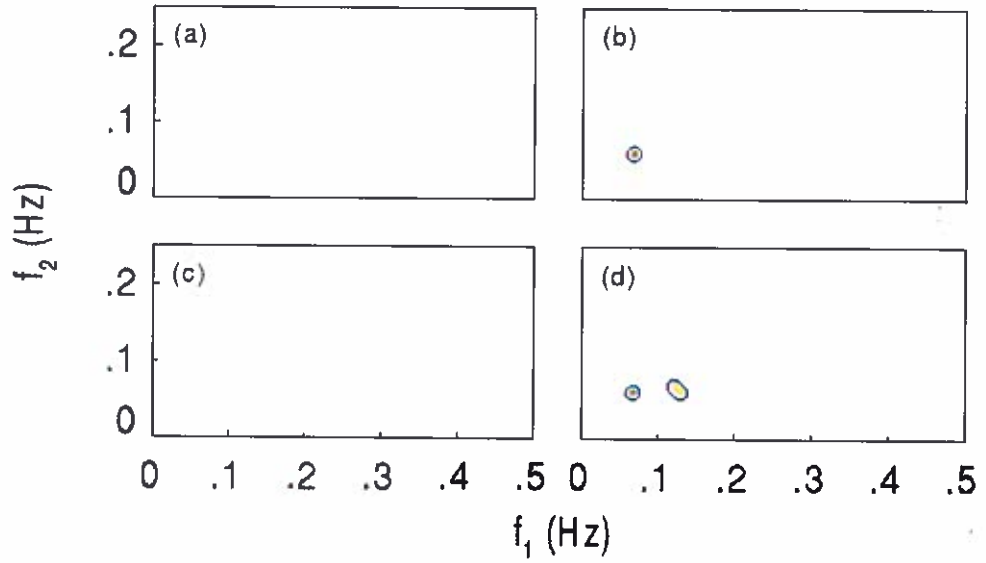

Fig. 6. Bicoherence spectra for the time series of Example 2. The format is the same as Fig. 3. (a) $\hat{b} = \hat{t} = 0$, (b) $\hat{b} = 0.9$, $\hat{t} = 0$, (c) $\hat{b} = 0$, $\hat{t} = 0.9$, (d) $\hat{b} = \hat{t} = 0.9$ (See text for complete description of the time series.)

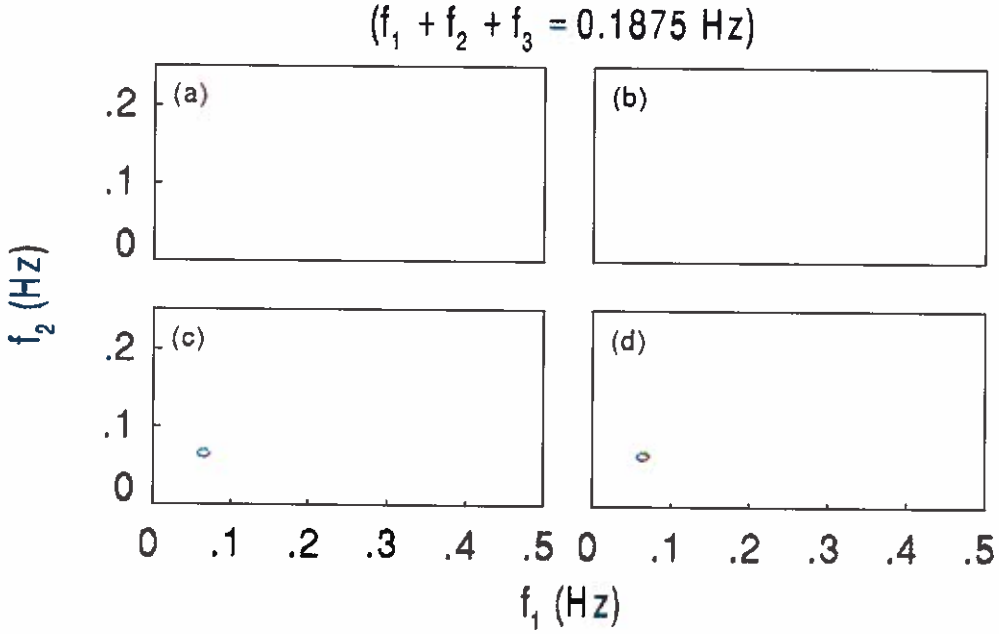

Fig. 7. Tricoherence spectra for the time series of Example 2. In each panel $f_4 = 0.1875$ Hz, and color contours indicate cubic phase coupling between motions with frequencies f_1, f_2, f_3, $f_4 = f_1 + f_2 + f_3$.(See Fig. 4 and accompanying text for a complete description of the format.) The minimum contour plotted is $t = 0.2$ and the scale for the contours is given by the color bar at the top of Fig. 3. (a) $\hat{b} = \hat{t} = 0$, (b) $\hat{b} = 0.9$, $\hat{t} = 0$, (c) $\hat{b} = 0$, $\hat{t} = 0.9$, (d) $\hat{b} = \hat{t} = 0.9$.

ies of the statistics of estimates of higher-order spectra. These are not reviewed in detail here. Haubrich [1965], Hinich & Clay [1968], Kim & Powers [1979], Elgar & Guza [1988], Elgar & Sebert [1989], Chandran & Elgar [1991], and others discuss the statistics of estimates of bicoherence and biphase. Statistical properties of trispectral estimates are discussed by Dalle Molle & Hinich [1989], Kim [1991], and Chandran *et al.* [1993b].

A 95% significance level on zero bicoherence is given by Haubrich [1965] as

$$b^2_{95\%} = 6/\text{d.o.f.} \tag{13}$$

where d.o.f. is the number of degrees of freedom used in the estimate of the bicoherence. Thus, there

is only a 5% chance that a bicoherence estimate would exceed this value if the process were truly Gaussian. Chandran *et al.* [1993b] demonstrate that this relationship holds for any higher-order coherence, and give expressions for other significance levels. Similarly, given an observed (i.e., estimated) higher-order coherence from a finite-length data record, the most likely true value can be determined using maximum likelihood techniques [Elgar & Sebert, 1989; Chandran *et al.*, 1993b]. Elgar & Sebert [1989] also discuss the statistical fluctuations associated with estimates of the biphase.

Similar to power spectral estimates, higher-order spectra are subject to corruption owing to spectral leakage [Subba Rao & Gabr, 1984; Chandran & Elgar, 1991] and/or smearing (owing to finite record lengths and smoothing to reduce statistical fluctuations). For the examples presented above, and for the analysis of the Chua circuit presented below, tests with different spectral windows and record lengths indicate that the conclusions based on the power spectra and higher-order spectra presented here are not significantly affected by leakage or smearing.

3. Higher-Order Spectra of Chua's Circuit

In this section higher-order spectral analysis is applied to data obtained from Chua's circuit [Matsumoto, 1984; Chua *et al.*, 1985]. In particular, a single state variable is analyzed as the system follows a period-doubling route to chaos to determine which Fourier components are interacting with each other. Higher-order spectra suggest that both quadratic and cubic nonlinear interactions are important during the period-doubling cascade. A chaotic state which results from this period-doubling cascade corresponds to a Rössler-like attractor. Although the Rössler equations are quadratically nonlinear [Thompson & Stewart, 1986 and references therein], while Chua's equation is piecewise-linear, bispectral analysis suggests that quadratic nonlinear modal interactions are important in both cases.

In contrast, the double-scroll chaotic attractor which appears in Chua's circuit [Chua *et al.*, 1985, Matsumoto *et al.*, 1985] is *not* dominated by quadratic nonlinearities, as demonstrated by low bicoherence values. On the other hand, tricoherence analysis suggests that cubic interactions play an important role in the double scroll.

3.1. *Chua's Circuit*

Chua's circuit (Fig. 8) consists of a linear inductor L, two linear capacitors C_1 and C_2, a linear resistor R, and a nonlinear resistor N_R. This circuit is described by a set of three ordinary differential equations [Chua *et al.*, 1985; Zhong & Ayrom, 1985]

$$\begin{aligned} C_1\frac{dv_{C_1}}{dt} &= G(v_{C_2}-v_{C_1})-g(v_{C_1})\,,\\ C_2\frac{dv_{C_2}}{dt} &= G(v_{C_1}-v_{C_2})+i_L\,,\\ L\frac{di_L}{dt} &= -v_{C_2}\,, \end{aligned} \tag{14}$$

where v_{C_1} and v_{C_2} are the voltages across capacitors C_1 and C_2 respectively, and i_L is the current flowing upwards through the inductor. G denotes the conductance of $R(G=1/R)$ and $g(\cdot)$ is a piecewise-linear function relating the current in the resistor $[g(v_R)]$ to the voltage (v_R):

$$g(v_R)=m_0v_R+0.5(m_1-m_0)(|v_R+B_p|-|v_R-B_p|)\,. \tag{15}$$

The slope of the current versus voltage curve changes from m_0 to m_1 when the voltage changes in absolute value from greater than B_p to less than B_p. Chua's circuit has been studied extensively both experimentally and analytically and exhibits every type of bifurcation and attractor reported for a third-order continuous time dynamical system (for a comprehensive bibliography of papers on Chua's circuit see Kennedy [1992a]).

Realizations of Chua's circuit can be obtained

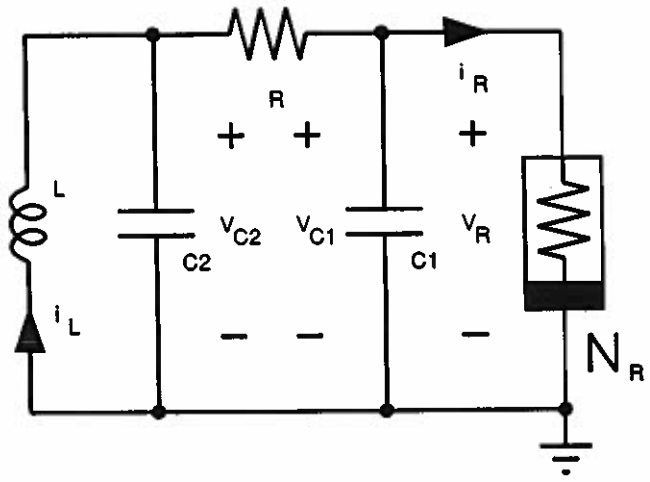

Fig. 8. Chua's circuit, consisting of a linear inductor, L, a linear resistor, R, two linear capacitors, C_1, C_2, and a nonlinear resistor, N_R. Dimensional values for the circuit parameters are given in the text.

using standard or custom-made components. While the linear elements are readily available as two-terminal devices, the nonlinear resistor (a Chua diode [Kennedy, 1992a]) must be constructed from active circuit elements. The implementation of Chua's circuit used in the present study is discussed in Kennedy [1992b] and Elgar & Kennedy [1993]. Here, N_R consists of a negative impedance converter and two ideal-diode subcircuits [Chua *et al.*, 1987] which determine the breakpoints $\pm B_p$ in the $v - i$ characteristic [Eq. (15)]. A complete list of the circuit elements used here is given in Elgar & Kennedy [1993]. The nonlinearity of the system is varied by fixing all components except the capacitance C_1. Larger values of C_1 correspond to greater nonlinearity. For the data discussed here, $C_2 = 178.5$ nF, $R = 1.001$ kΩ, $L = 12.44$ mH, $B_p = 1$ V, $m_0 = -0.712$, and $m_1 = -1.14$.

3.2. *Experimental results for Chua's circuit*

A period-doubling sequence and two chaotic states, corresponding to a Rössler attractor (a model of the Lorenz attractor, Thompson & Stewart [1986] and references therein) and to the double scroll [Chua *et al.*, 1985, Matsumoto *et al.*, 1985] were examined.

Five time series of the voltage waveform v_{C_1} for five different values of the capacitance C_1 (Table 1) were recorded. Analog-to-digital conversion was achieved by means of a 16-bit data acquisition board with fourth-order lowpass (20 kHz corner frequency) filters. The data acquisition board was preceded by an amplifier whose gain was adjusted to match the signal level to the input dynamic range of the convertor. The sampling frequency was 49.9 kHz.

Table 1. Values of C_1 for the five case studies of the Chua circuit discussed in the text.

Case	$C_1(nF)$
Period 1	17.5
Period 2	17.2
Period 4	16.9
Rössler	16.6
Double scroll	15.0

Power and higher-order spectra were calculated by subdividing the voltage time series into 384 short records, each 256 points long. A Hanning window with 75% overlap was applied to each short time series to reduce spectral leakage, and power and higher-order spectra from each of the 384 records were ensemble averaged producing estimates with about 768 degrees of freedom and a final frequency resolution of 0.195 kHz. There are several sources of noise in these data. The circuit elements are not perfect and both the analog to digital conversion and finite-word length computations cause some truncation (roundoff) of the signal. Nevertheless, although the data from the Chua circuit are measured voltages, the noise levels are extremely low. In a deterministic system there are no random phase relationships between the Fourier components, and all higher-order coherences are 1. In the presence of very low background noise, spectral leakage owing to finite record lengths can result in artifically

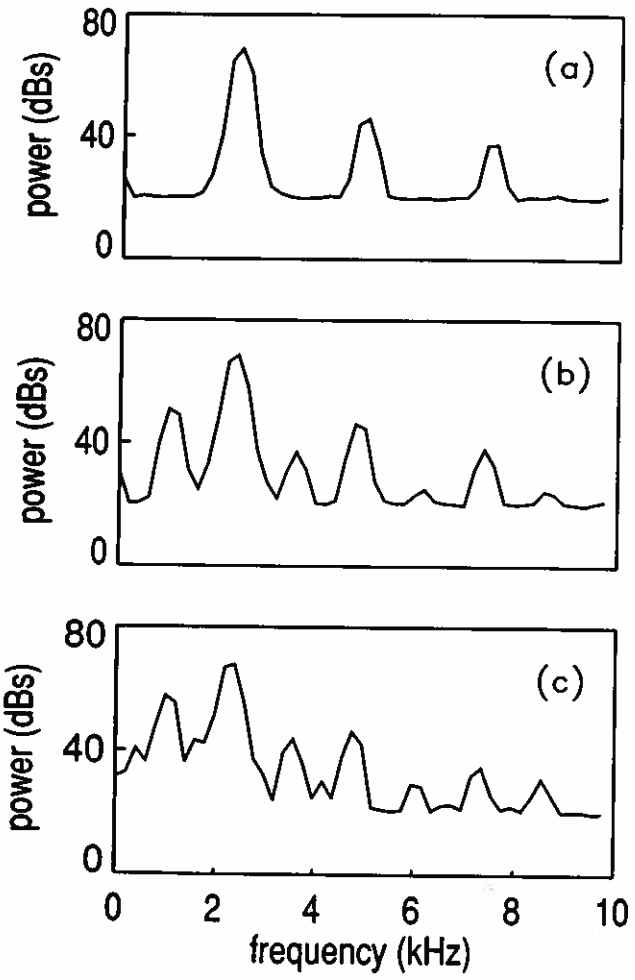

Fig. 9. Power spectra of voltage v_{C_1} measured from Chua's circuit. (a) period-1 limit cycle, (b) period-2 limit cycle, and (c) period-4 limit cycle. The corresponding values of the capacitance, C_1 are given in Table 1. The units of power are arbitrary.

large higher-order coherences for Fourier triads and quartets with one or more very low energy components. Both to avoid such artifacts and to demonstrate the power of higher-order spectral analysis to detect nonlinear interactions in a random process with significant background noise, Gaussian noise (less than 2% of the total variance) was added to the measured voltages for the cases discussed below.

The harmonic structure of the limit cycles is clearly displayed in the power spectra (Fig. 9), which are characterized by narrow peaks. For period-1 motion, the spectrum is dominated by a primary spectral peak with frequency $f = 2.5$ kHz, and its higher harmonics. As C_1 is increased, the subharmonic ($f = 1.25$ kHz) is excited [period-2 motion, Fig. 9(b)] and, owing to nonlinear interactions the spectrum contains peaks at frequencies corresponding to sum interactions of the subharmonic, the primary, and their harmonics. As C_1 is increased further, another period-doubling occurs ($f = 0.625$ kHz is excited, period-4 motion), and the power spectrum [Fig. 9(c)] contains many peaks, corresponding to the two subharmonics, the primary, and their combination tones.

The quadratic and cubic interactions between triads of Fourier components for the limit cycles of Chua's circuit are isolated by bicoherence and tricoherence spectra (Figs. 10 and 11). For the period-1 case, bicoherence spectra clearly show the quadratic coupling between motions at the primary spectral peak frequency and its harmonics [$f_1 = 2.5$, $f_2 = 2.5$ and $f_1 = 5.0$, $f_2 = 2.5$ kHz, Fig. 10(a)]. The high bicoherence values associated with $f_2 = 2.5$ kHz [Fig. 10(a)] indicate nonlinear energy transfer from the primary to higher-frequency components. The quadratic interactions are restricted to triads of Fourier components that include the primary and its harmonics. Cubic interactions also occur for period-1 motion, as shown in Fig. 11, and there is strong coupling among the quartet of components consisting of $f_1 = f_2 = f_3 = 2.5$ and $f_4 = 7.5$ kHz [Fig. 11(d)], a self-self cubic interaction transferring energy from motions at the power spectral peak frequency ($f = 2.5$ kHz) to those at three times the peak frequency ($f = 7.5$ kHz), as well as between the primary and higher harmonics [e.g., $f_1 = 5$, $f_2 = 2.5$, $f_3 = 2.5$, $f_4 = 10$ kHz, Fig. 11(g)].

Power spectra for the period-2 case [Fig. 9(b)] show narrow peaks between the harmonics of the primary peak. The corresponding bicoherence spectrum [Fig. 10(b)] shows the coupling between motions at the primary peak frequency ($f = 2.5$ kHz), its harmonics, the period-doubled frequency (subharmonic, $f = 1.25$ kHz), and its harmonics. Quadratic interactions between oscillations at the primary and the period-doubled subharmonic are transferring energy into higher harmonics. Similarly, there are strong cubic interactions between the subharmonic and the primary [Fig. 11(b)], as well as between the subharmonic and higher frequency motions (the range of significant tricoherences for period-2 motion, $f_4 = 7.5$ and $f_4 = 10$ kHz [Figs. 11(e), (h)] include more low frequency components than the period-1 motion tricoherences [Figs. 11(d), (g)].

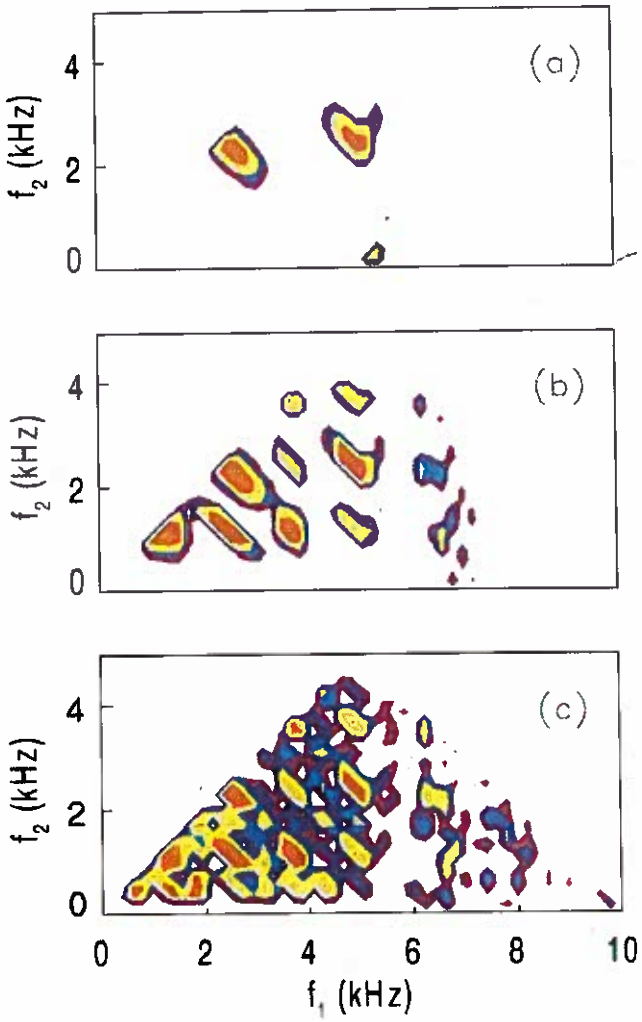

Fig. 10. Bicoherence spectra of voltage v_{C_1} measured from Chua's circuit. (a) period-1 limit cycle, (b) period-2 limit cycle, and (c) period-4 limit cycle. The format is the same as Fig. 3.

For period-4 motion an additional subharmonic is excited ($f = 0.625$ kHz), and the power [Fig. 9(c)], bicoherence [Fig. 10(c)], and tricoher-

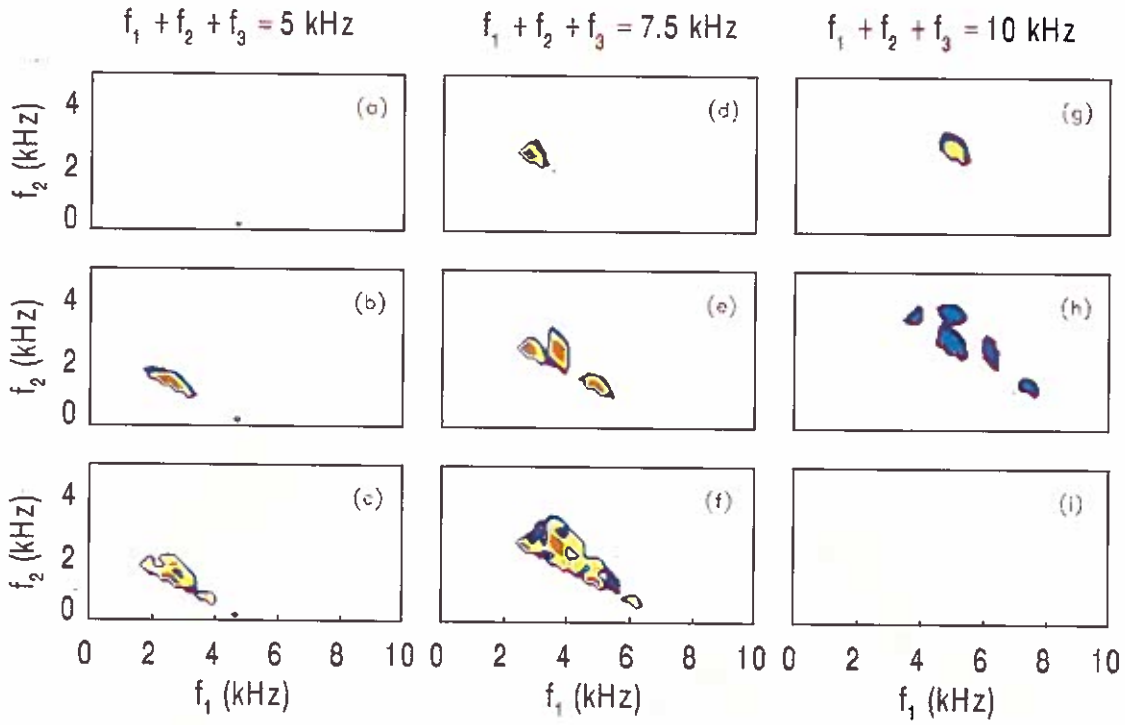

Fig. 11. Tricoherence spectra of voltage v_{C_1} measured from Chua's circuit. The rows of panels are [top, (a, d, g)] period-1 limit cycle, [middle, (b, e, h)] period-2 limit cycle, and [bottom (c, f, i)] period-4 limit cycle. The columns are for constant sum frequencies [left (a, b, c)] $f_4 = 2.5$, [center (d, e, f)] $f_4 = 5$, and [right (g, h, i)] $f_4 = 10$ kHz. The format of each panel is the same as Fig. 7.

ence [Figs. 11(c), (f), (i)] spectra contain peaks associated with the primary ($f = 2.5$ kHz), both subharmonics ($f = 1.25$ kHz and $f = 0.625$ kHz), and all their combination tones. The higher-order spectra indicate that these interactions are quadratic and cubic, and delineate precisely which Fourier components are interacting with each other.

Time series corresponding to the Rössler attractor exhibit similarities to, and differences from, the period-doubling sequences shown in Figs. 9–11. The Rössler-like attractor is chaotic and has a fairly broad power spectrum [Fig. 12(a)] with only remnants of the sharp primary and harmonic peaks of the period-doubled cases [Fig. 9]. However, as can be seen in the bicoherence [Fig. 12(b)] and tricoherence (Fig. 13) spectra, both quadratic and cubic interactions are still important. Motions corresponding to the remnant of the primary peak ($f_2 = 2.5$ kHz) are quadratically coupled to both higher frequencies [horizontal band of contours at $f_2 = 2.5$ kHz in Fig. 12(b)] and to lower frequencies (vertical band of contours at $f_1 = 2.5$ kHz). Weaker quadratic interactions occur between motions at the harmonics ($f = 5.0$ and $f = 7.5$ kHz) of the primary spectral peak and both higher- and lower-frequency motions. Bicoherences are statistically significant for many frequency triads, indicating that quadratic nonlinear interactions occur between nearly all the frequency components of the Rössler system. Cubic nonlinear interactions (Fig. 13), although individually weaker than the quadratic interactions are also important in the Rössler attractor, and occur between nearly all the components of the system.

Unlike the period-doubled and Rössler attractors, the double scroll is not dominated by quadratic interactions. The double-scroll attractor is characterized by a very broad power spectrum [Fig. 14(a)], with only a vestige of the primary peak ($f = 2.5$ kHz) and much more energetic low-frequency motions [compare Fig. 14(a) to Figs. 9 and 12(a)]. There are no statistically significant bicoherences [Fig. 14(b)], indicating that the nonlinearities for the double scroll are not quadratic. A Rössler-type attractor in Chua's circuit is confined to two regions of the piecewise-linearity. In contrast, trajectories in the double scroll visit all three regions. While a two-segment nonlinearity can be approximated by a quadratic, the three-segment nonlinearity requires a higher-order approximation. Since the motion is global in nature, the absolute value term dominates the motion, thus leaving only an insignificant amount of quadratic phase coupling and energy transfer in the system's motion. Similar behavior

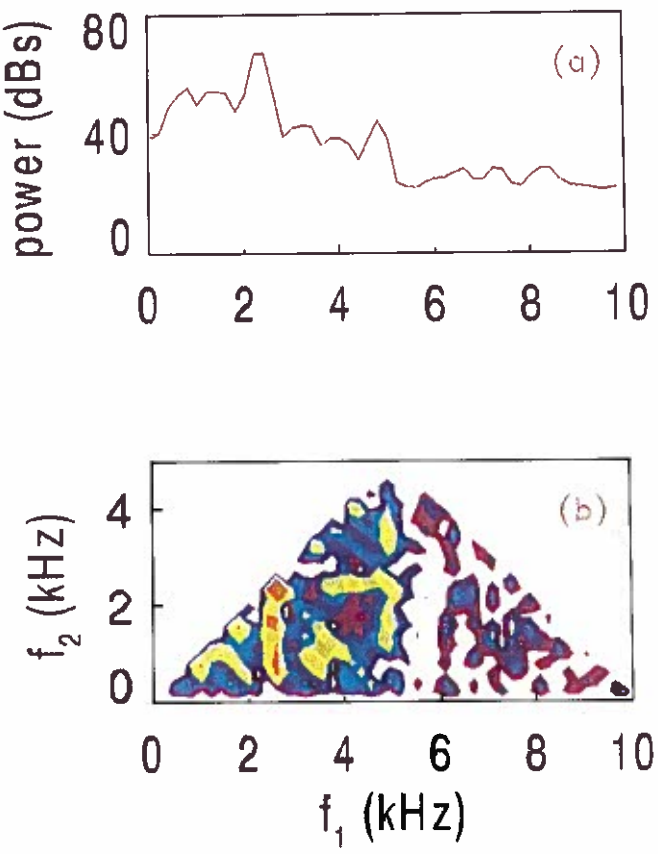

Fig. 12. (a) Power spectrum and (b) contours of bicoherence of voltage v_{C_1} measured from Chua's circuit when the system exhibits a Rössler-like attractor. The units of power are arbitrary and the format of the bicoherence spectrum is the same as Fig. 3.

has been observed in the driven Sine–Gordon chain [Miller, 1986] and the Duffing equation [Pezeshki *et al.*, 1990; Chandran *et al.*, 1993a]. Higher-than-second order spectra are required to isolate the individual interacting Fourier components for the double scroll. As shown by the tricoherence spectra (Fig. 15), although the strength of individual cubic interactions is not as great as in some of the cases discussed above, many of the Fourier components of the double-scroll system are cubically coupled to each other. Tricoherence spectra suggest that interactions involving low frequency components are important to the dynamics of the double scroll (i.e., there are many cubically coupled triads involving low frequencies for the double scroll, as shown in Fig. 15). Similar importance of nonlinear interactions involving very low frequency components has been observed in other chaotic systems [Miksad *et al.*, 1983; Elgar *et al.*, 1989; Pezeshki *et al.*, 1990; Chandran *et al.*, 1993a, and others].

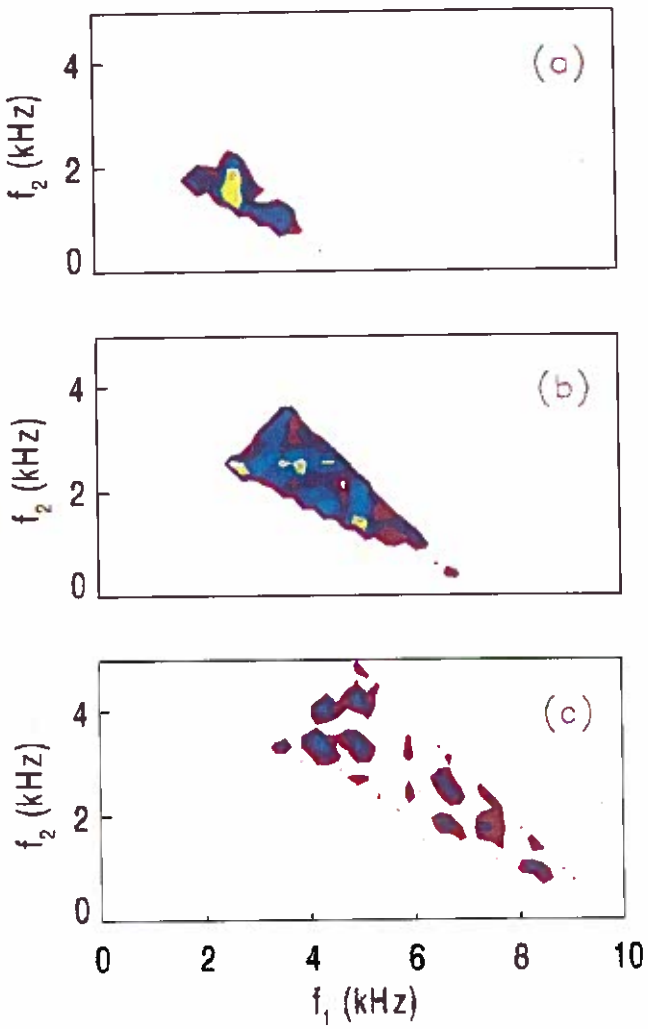

Fig. 13. Tricoherence spectra of voltage v_{C_1} measured from Chua's circuit when the system exhibits a Rössler-like attractor. The constant sum frequencies are (a) $f_4 = 2.5$, (b) $f_4 = 5$, and (c) $f_4 = 10$ kHz.

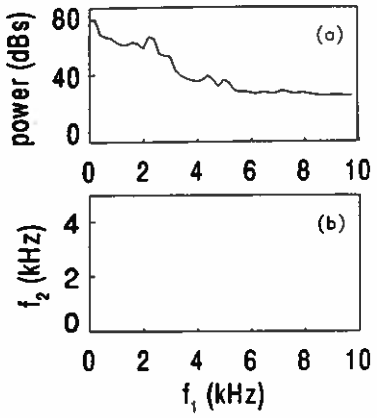

Fig. 14. (a) Power spectrum and (b) contours of bicoherence of voltage v_{C_1} measured from the double-scroll attractor in Chua's circuit. The units of power are arbitrary and the format of the bicoherence spectrum is the same as Fig. 3.

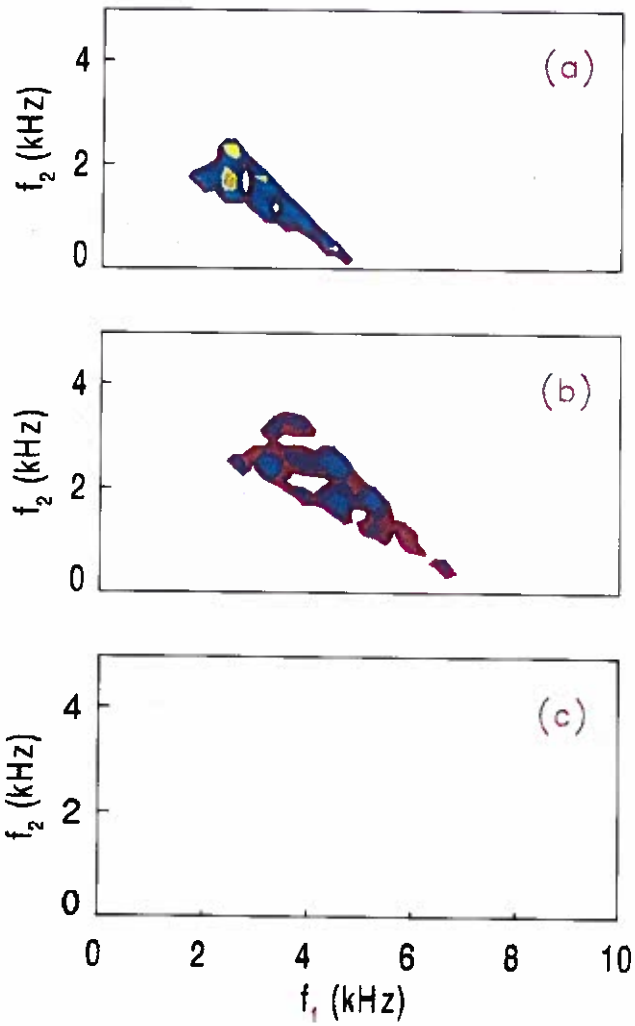

Fig. 15. Tricoherence spectra of voltage v_{C_1} measured from the double-scroll attractor in Chua's circuit. The constant sum frequencies are (a) $f_4 = 2.5$, (b) $f_4 = 5$, and (c) $f_4 = 10$ kHz.

4. Conclusions

Higher-order spectral analysis detects and isolates the phase coupling caused by nonlinear interactions between the Fourier components of a random process. Quadratic nonlinear interactions between triads of components are detected by bispectra and cubic interactions between quartets of components are detected by trispectra. Higher-order spectra are zero for linear and/or Gaussian processes and, thus, reject background noise. Consequently, higher-order spectra provide information about nonlinear systems in addition to that provided by the power spectrum and phase portraits (and associated measures).

Higher-order spectral analysis of time series of voltages measured in a realization of Chua's circuit, a canonical nonlinear dynamical system, isolate the individual nonlinear interactions between the many Fourier components of the system. As Chua's circuit undergoes a period-doubling sequence to chaos quadratic and cubic nonlinear interactions couple, and transfer energy between, triads and quartets of Fourier components. The individual interactions are isolated by bicoherence and tricoherence spectra, which show increasing numbers of phase coupled components as the nonlinearity of the system is increased. For a period-1 limit cycle, motions at the frequency corresponding to the power spectral peak frequency and its harmonics are coupled. For a period-2 limit cycle, motions at the subharmonic, the primary, and their super harmonic frequencies are coupled, while for period-4 motion the many combinations of lowest subharmonic, subharmonic, primary, and corresponding super harmonics are nonlinearly coupled.

When the system becomes chaotic the power spectrum broadens, but in the case of the Rössler attractor, quadratic and cubic nonlinear interactions remain important. Motions at the primary frequency and its harmonics are coupled to motions at many other frequencies. For the double-scroll attractor the system no longer contains quadratic nonlinear interactions, and bicoherence values are essentially zero. However, tricoherence spectra demonstrate the continued importance of cubic nonlinear interactions.

Acknowledgments

Our research on higher-order spectra, especially for investigating observations of ocean waves, has been generously supported by the Office of Naval Research (Coastal Sciences, NOW ARI, and Geology & Geophysics) and the National Science Foundation (Physical Oceanography). Additional support was provided by the Dirección General de Investigación Científica y Técnica of Spain. The generosity of Dr. C. D. Winant (Center for Coastal Studies) and Dr. J. Medina (Universidad Politécnica de Valencia) while this manuscript was being prepared is warmly and gratefully acknowledged. We thank Dr. Leon Chua for suggesting the application of higher-order spectral analysis to the Chua circuit. Our work with higher-order spectra has benefitted tremendously by conversations and collaborations with M. Freilich, M. Gharib, R. Guza, T. Herbers, T. Hagelberg, M. Kennedy, W. Munk, C. Pezeshki, G. Sebert, C. Van Atta, B. Vanhoff, and others. We are grateful to Chai

Wah Wu of U.C. Berkeley for his assistance in acquiring the experimental data from the Chua circuit.

References

Arter, W. & Edwards, D. N. [1986] "Nonlinear studies of Mirnov oscillations in the DITE Tokamak: Evidence for a strange attractor," *Phys. Lett.* **A114**, 84–89.

Barnett, T. P., Johnson, L. C., Naitoh, P., Hicks, N. & Nute, C. [1971] "Bispectrum analysis of electroencephalogram signals during waking and sleeping," *Science* **172**, 401–402.

Bartelt, H. & Wirnitzer, B. [1985] "Shift-invariant imaging of photon-limited data using bispectral analysis," *Opt. Commun.* **53**, 13–16.

Brillinger, D. [1965] "An introduction to polyspectra," *Ann. Math. Statist.* **36**, 1351–1374.

Brillinger, D. & Rosenblatt, M. [1967a] "Asymptotic theory of kth-order spectra," in *Advanced Seminar on Spectral Analysis of Time Series* ed. B. Harris (Wiley), pp. 153–188.

Brillinger, D. & Rosenblatt, M. [1967b] "Computation and interpretation of kth-order spectra," in *Advanced Seminar on Spectral Analysis of Time Series* ed. B. Harris (Wiley), pp. 189–232.

Brandstater, B. & Swinney, H. L. [1987] "Strange attractors in weakly turbulent Couette–Taylor flow," *Phys. Rev.* **A35**, 2207–2220.

Chandran, V. & Elgar, S. [1990] "Bispectral analysis of 2-D random processes," *IEEE Acoustics, Speech, and Signal Processing*, **38**, 2181–2186.

Chandran, V. & Elgar, S. [1991] "Mean and variance of estimates of the bispectrum of a harmonic random process: An analysis including effects of spectral leakage," *IEEE Signal Processing*, **39**, 2640–2651.

Chandran, V. & Elgar, S. [1993a] "Pattern recognition using invariants defined from higher-order spectra: One-dimensional inputs," *IEEE Acoustics, Speech, and Signal Processing*, in press.

Chandran, V. & Elgar, S. [1993b] "A general procedure for the derivation of principal domains of higher-order spectra," *IEEE Signal Processing*, in press.

Chandran, V., Elgar, S., & Pezeshki, C. [1993a] "Bispectral and trispectral characterization of transition to chaos in the Duffing oscillator," submitted to *Int. J. Bifurcation and Chaos.*

Chandran, V., Elgar, S. & Vanhoff, B. [1993b] "Statistics of tricoherence," submitted to *IEEE Signal Processing.*

Chua, L., Komuro, M. & Matsumoto, T. [1985] "The double scroll family," *IEEE Circuits and System* **33**, 1073–1118.

Chua, L., Desoer, C. & Kuh, E. [1987] *Linear and nonlinear circuits* (New York, McGraw-Hill).

Choi, D., Miksad, R. W. & Powers, E. J. [1985] "Application of cross-bispectral analysis techniques to model the nonlinear response of a moored vessel system in random seas," *J. Sound and Vibration* **99**, 309–326.

Dalle Molle, J. W. [1992] "Higher-order spectral analysis and the trispectrum," Ph.D. Dissertation, University of Texas, Austin, TX. 116 pp.

Dalle Molle, J. W. & Hinich, M. J. [1989] "The trispectrum," *Proceedings of the Workshop on HOS Analysis* (ed. J. Mendel and C. Nikias), Vail, CO., 68–71.

Dwyer, R. F. [1984] "Use of kurtosis in the frequency domain as an aid in detecting random signals," *IEEE J. Ocean Engineering* **9**, 85–92.

Dwyer, R. F. [1989] "Fourth-order spectra of sonar signals," *Proceedings of the Workshop on HOS Analysis* (ed. J. Mendel and C. Nikias), Vail, CO., 52–55.

Elgar, S. [1987] "Relationships involving third moments and bispectra of a harmonic process," *IEEE Acoustics, Speech, and Signal Processing*, **35**, 1725–1726.

Elgar, S. & Guza, R. T. [1985] "Observations of bispectra of shoaling surface gravity waves," *J. Fluid Mechanics*, **161**, 425–448.

Elgar, S. & Guza, R. T. [1988] "Statistics of bicoherence," *IEEE Acoustics, Speech, and Signal Processing*, **36**, 1667–1668.

Elgar, S. & Sebert, G. [1989] "Statistics of bicoherence and biphase," *J. Geophysical Research* **94**, 10993–10998.

Elgar, S. & Kennedy, M. P. [1993] "Bispectral analysis of Chua's circuit," *J. Circuits, Systems, and Computers*, in press.

Elgar, S., Van Atta, C. W. & Gharib, M. [1989] "Bispectral analysis of ordered and chaotic vortex shedding from vibrating cylinders, " *Physica* **D39**, 281–286.

Elgar, S., Van Atta, C. W. & Gharib, M. [1990] "Cross-bispectral analysis of the coupling between a vibrating cylinder and its wake in low Reynolds number flow," *J. Fluids and Structures* **4**, 59–71.

Farmer, J., Ott, E. & Yorke, J. [1983] "The dimension of chaotic attractors," *Physica* **D7**, 153–179.

Frederickson, P., Kaplan, J., Yorke, E. & Yorke, J. [1983] "The Lyapunov dimension of strange attractors," *J. Differential Equations* **49**, 185–207.

Godfrey, M. D. [1965] "An exploratory study of the bispectrum of economic time series," *Appl. Statist.* **14**, 48–69.

Grassberger, P. & Procaccia, I. [1983a] "Characterization of strange attractors," *Phys. Rev. Lett.* **50**, 346–349.

Grassberger, P. & Procaccia, I. [1983b] "Measuring the strangeness of strange attractors," *Physica* **D9**, 189–208.

Hagelberg, T., Pisias, N. & Elgar, S. [1991] "Linear and nonlinear coupling between orbital forcing and the marine $\delta^{18}O$ record during the late Neogene," *Paleoceanography* **6**, 729–746.

Hajj, M., Miksad, R. & Powers, E. J. [1992] "Subharmonic growth by parametric resonance," *J. Fluid Mechanics* **236**, 385–413.

Hasselmann, K., Munk, W. & MacDonald, G [1963] "Bispectra of ocean waves," in *Time Series Analysis*, ed. M. Rosenblatt (John Wiley, New York), pp. 125–139.

Haubrich, R. A. [1965] "Earth noises, 5 to 500 millicycles per second," *J. Geophysical Research* **70**, 1415–1427.

Helland, K. N., Van Atta, C. W. & Stegun, G. N. [1977] "Spectral energy transfer in high Reynolds number turbulence," *J. Fluid Mech.* **79**, 337–359.

Herbers, T. H. C. & Guza, R. T. [1992] "Wind wave nonlinearity observed at the sea floor, Part II: Wave numbers and third-order statistics," *J. Physical Oceanography* **22**, 489–504.

Herbers, T. H. C., Lowe, R. L. & Guza, R. T. [1992] "Field observations of orbital velocities and pressure in weakly nonlinear surface gravity waves," *J. Fluid Mech.* **245**, 413–435.

Herbers, T. H. C., Elgar, S. & Guza, R. T. [1993] "Infragravity-frequency (0.005–0.05 Hz) motions on the shelf, Part I: Local nonlinear forcing by surface waves," submitted to *J. Physical Oceanography.*

Herring, J. R. [1980] "Theoretical calculations on turbulent bispectra." *J. Fluid Mech.* **97**, 193–204.

Hinich, M. J. & Clay, C. S. [1968] "The application of the discrete Fourier transform in the estimation of power spectra, coherence, and bispectra of geophysical data," *Reviews of Geophysics* **6**, 347–363.

Hinich, M. J. & Patterson, D. M. [1989] "Evidence of nonlinearity in the trade-by-trade stock market return generating process," in *Chaos, Sunspots, Bubbles, and Nonlinearity*, ed. by W. A. Barnett, J. Geweke, and K. Shell (Cambridge University Press, New York), pp. 383–409.

Hinich, M. J., Maradino, D. & Sullivan, E. J. [1989] "Bispectrum of ship radiated noise," *J. Acoustical Society of America* **85**, 1512–1517.

Huber, P. J., Kleiner, B. Gasser, T. & Dumermath, G. [1971] "Statistical methods for investigating phase relations in stationary stochastic process," *IEEE Trans. Audio and Electroacoustics*, **19**, 78–86.

Kennedy, M. P. [1992a] "Robust Op Amp realization of Chua's circuit," *Frequenz* **46**, 66–88.

Kennedy, M. P. [1992b] "Design notes for Chua's circuit," *Electronics Research Laboratory Memorandum* (University of California, Berkeley).

Kim, P. T. [1991] "Consistent estimation of the fourth-order cumulant spectral density," *J. Time Series Analysis* **12**, 63–71.

Kim, Y. C. & Powers, E. J. [1978] "Digital bispectral analysis of self-excited fluctuation spectra," *Physics of Fluids.* **21**, 1452–1453.

Kim, Y. C. & Powers, E. J. [1979] "Digital bispectral analysis and its applications to nonlinear wave interactions," *IEEE Trans. Plasma Science* **7**, 120–131.

Kim, Y. C., Beall, J. M., Powers, E. J. & Miksad, R. W. [1980] "Bispectrum and nonlinear wave coupling," *Physics of Fluids* **21**(8), 258-263.

Lii, K. S. & Helland, K. N. [1981] "Cross bispectrum computation and variance estimation," *ACM Transactions Math Software* **7**, 284–294.

Lii, K. S., Rosenblatt, M. & Van Atta, C. W. [1976] "Bispectral measurements in turbulence," *J. Fluid Mech.* **77**, 45–62.

Lutes, L. D. & Chen, D. C. K. [1991] "Trispectrum for the response of a nonlinear oscillator," *Internat. J. Nonlinear Mechanics* **26**, 893–909.

Lohmann, A. W., Weigelt, G. P. & Wirnitzer, B. [1983] "Speckle masking in astronomy–Triple correlation theory and applications," *Applied Optics* **22**, 4028–4037.

Masuda, A. & Kuo, Y. [1981a] "A note on the imaginary part of the bispectrum," *Deep Sea Research* **28**, 213–222.

Masuda, A. & Kuo, Y. [1981b] "Bispectra for the surface displacement of random gravity waves in deep water," *Deep Sea Research* **28**, 233–237.

Matsumoto, T. [1984] "A Chaotic attractor from Chua's Circuit," *IEEE Circuits and Systems* **31**, 1055–1058.

Matsumoto, T., Chua, L. & Komuro, M. [1985] "The double scroll," *IEEE Circuits and Systems* **33**, 798–818.

McComas, C. & Briscoe, M. [1980] "Bispectra of internal waves," *J. Fluid Mech.* **97**, 205–213.

Mendel, J. [1991] "Tutorial on higher-order statistics (spectra) in signal processing and system theory: Theoretical results and some applications," *Proceedings of the IEEE* **79**, 278–305.

Miksad, R. W., Jones, F. & Powers, E. J. [1983] "Measurements of nonlinear interactions during natural transition of a symmetric wake," *Physics of Fluids* **26**, 1402–1408.

Miles, W. H., Pezeshki, C. & Elgar, S. [1992] "Bispectral analysis of a fluid elastic system; the cantilevered pipe," *J. Fluids and Structures* **6**, 633–640.

Miller, M. D. [1986] "Bispectral analysis of the driven Sine–Gordon chain," *Phys. Rev.* **B34**, 6326–6333.

Neshyba, S. & Sobey, E. J. C. [1975] "Vertical cross coherence and cross bispectra between internal waves measured in a multiple-layered ocean," *J. Geophysical Research* **80**, 1152–1162.

Nikias, C. L. & Raghuveer, M. R. [1987] "Bispectrum estimation: A digital signal processing framework," *Proceedings of IEEE* **75**, 869–891.

Packard, N., Crutchfield, J., Farmer, D. & Shaw, R. [1980] "Geometry from a time series," *Phys. Rev. Lett.* **45**, 712–715.

Pezeshki, C., Elgar S. & Krishna, R. C. [1990] "Bispectral analysis of systems possessing chaotic motion," *J. Sound Vibration* **137**, 357–368.

Pezeshki, C., Elgar, S. & Krishna, R. C. [1991] "An examination of multifrequency excitation of the buckled beam," *J. Sound Vibration* **148**, 1–9.

Pezeshki, C., Elgar, S., Krishna, R. C. & Burton, T. D. [1992] "Auto- and cross-bispectral analysis of a system of two coupled oscillators with quadratic nonlinearities

possessing chaotic notion," *J. Appl. Mech.* **59**, 657–663.

Raghuveer, M. R. & Dianat, S. A. [1988] "Detection of nonlinear phase coupling in multidimensional stochastic processes," *Proc. Int. Conference on Advances in Control and Communication*, 729–732.

Ritz, C., Powers, E. J., Miksad, R. W. & Solis, R. [1988] "Nonlinear spectral dynamics of a transitioning flow," *Physics of Fluids* **31**, 3577–3588.

Rodin, G. I. & Bendiner, D. J. [1973] "Bispectra and cross bispectra of temperature, salinity, sound velocity, and density fluctuations with depth off Northeastern Japan," *J. Physical Oceanography* **3**, 308–317.

Rosenblatt, M. & Van Ness J. W. [1965] "Estimation of the bispectrum," *Ann. Math. Statist.* **36**, 1120–1136.

Roux, J. O., Simoyi, R. H. & Swinney, H. L. [1983] "Observation of a strange attractor," *Physica* **D8**, 257–266.

Sadler, B. M. [1989] "Shift and rotation invariant object reconstruction using the bispectrum," *Proceedings of the Workshop on HOS Analysis* (ed. J. Mendel and C. Nikias), Vail, CO. 106–111.

Sato, T., Sasaki, K. & Nakamura, Y. [1977] "Real-time bispectral analysis of gear noise and its application to contactless diagnosis," *J. Acoust. Soc. Amer.* **62**, 382–387.

Subba Rao, T. & Gabr, M. [1984] "An introduction to bispectral analysis and bilinear time series models," *Lecture Notes in Statistics* **24**, Springer, New York.

Thompson, J. B. & Stewart, H. B. [1986] *Nonlinear Dynamics and Chaos* (John Wiley, New York), pp. 235–238.

Van Atta, C. W. [1979] "Inertial range bispectra in turbulence," *Physics of Fluids* **22**, 1440–1443.

Wolf, A., Swift, J. B., Swinney, H. L. & Vastano, J. A. [1985] "Determining Lyapunov exponents from a time series," *Physica* **D16**, 285–317.

Yeh, T. T. & Van Atta, C. W. [1973] "Spectral transfer of scalar and velocity fields in heated-grid turbulence," *J. Fluid Mech.* **58**, 233–261.

Zhong, G. & Ayrom, F. [1985] "Experimental confirmation of chaos in Chua's circuit," *Internat. J. Circuit Theory Appl.* **13**, 93–98.